The Solubility of Gases in Polyethylene: Integral Equation Study of Standard Molecular Models

Joanne L. Budzien and John D. McCoy*

Department of Materials and Metallurgical Engineering, New Mexico Institute of Mining and Technology, Socorro, New Mexico 87801

John G. Curro

Sandia National Laboratories,† Albuquerque, New Mexico 87185

Randall A. LaViolette and Eric S. Peterson

Idaho National Engineering and Environmental Laboratory,‡ P.O. Box 1625, Idaho Falls, Idaho 83415

Received March 5, 1998; Revised Manuscript Received July 10, 1998

ABSTRACT: The solubility coefficients of a wide range of gases in polyethylene were calculated with a recently developed integral equation theory of gas solubility. Standard Lennard-Jones potential interactions were used for united atom models of both gas molecules and polyethylene, CH_2, sites. The cross interactions were assumed to be given by the standard Bertholet relationships, and care was taken to stay within the Henry's law limit. The predictions of the theory for the solubility of low critical temperature gases in polyethylene were compared to the experimental values. The agreement was excellent, and for the cases considered, there was no justification for introducing non-Bertholet cross interactions. On the other hand, the results were found to be sensitive to the details of the CH_2-CH_2 interaction.

1. Introduction

A methodology for the prediction of gas solubility in polymers[1] based upon the polymer reference interaction site model (PRISM) theory[2] was recently developed. In this theory, the chemical potential of the dilute gas in the polymer melt is treated as the sum of an entropic and an enthalpic contribution. The entropic term is calculated from the "growing" of a gas atom from a randomly inserted point particle. Perturbation theory then provides the enthalpic contribution. In both cases, the pair correlation function is required and is provided by PRISM theory. This approach is similar to scaled particle theory[3] except that the atomic pair correlation function arises from semiempirical hard sphere results while chain molecules require a molecular theory such as PRISM.

This treatment of gas solubility was found[1] to be exceedingly successful at predicting the qualitative behavior of the solubility of noble gases in polyethylene. A reasonable, but nonstandard, model for site−site interactions in polyethylene was used along with the classic "second virial coefficient" interaction potentials[4] for the gases. The room temperature solubility coefficients were shown to be in reasonable agreement with experimental measurements in natural rubber. More importantly, the relatively complex temperature behavior of the solubility coefficients was correctly described: the solubility coefficient of a gas increases with increasing temperature for gases with low critical temperatures and decreases with increasing temperature for gases with high critical temperatures.

The quantitative limits of the PRISM theory of gas solubility were not, however, explicitly probed in this earlier study for a number of reasons. First, experimental measurements of gas solubility coefficients are generally conducted at room temperature where polyethylene is not completely amorphous. Consequently, it was assumed that gas solubilities in natural rubber are similar to those in polyethylene. Recently, a new extrapolation[5] of experimental measurements to the amorphous limit has, along with a previous prediction,[6] confirmed this supposition. In the current study, PRISM predictions were compared to these new "experimental" predictions for polyethylene as well as to those for natural rubber.

Second, a wide range of CH_2-CH_2 interaction potentials exist,[7] which have been calibrated to the equation of state and other standard measures of accuracy. While it is true that the united atom nature of the potentials may introduce unexpected temperature dependencies,[7] the potentials are usually calibrated at or near room temperature, and there is merit in using such potentials in a study of room temperature polyethylene. In the current study, we have considered two recently developed potentials for comparisons with experimental results: the NERD potential of Nath, Escobedo, and de Pablo[8] and the TRaPPE potential of Martin and Siepmann.[9]

Finally, in order for a theory of gas solubility to be broadly useful in an industrial context, gases beyond noble ones must be addressed. While it is conceivable to explicitly treat the molecular nature of more complex gases within the PRISM context, there is a long history[4] of modeling molecular gases as single Lennard-Jones particles. In the current study, we have investigated a number of nonspherical gases in this manner, while

* To whom mail should be addressed.

† Work performed at Sandia National Laboratories supported by the U.S. Department of Energy under Contract No. DE-AC04-94AL85000.

‡ Work performed at Idaho National Engineering and Environmental Laboratory supported by the U.S. Department of Energy under Contract No. DE-AC04-94ID13223.

S0024-9297(98)00353-2 CCC: $15.00
Published on Web 08/27/1998

avoiding the more extreme cases. The spherical and nearly spherical gases chosen were, in order of increasing critical temperature (T_c), nitrogen, argon, oxygen, methane, krypton, xenon, carbon dioxide, and ethane.

More generally, since the solubility of gases in polymers is relatively easy to measure in both experiments[10] and simulations,[11,12] a good avenue for testing the accuracy of the underlying molecular models is provided by theories of gas solubility. This approach is particularly sensitive to details of the polymer−gas interaction, a quantity rarely addressed in more standard benchmarks such as the equation of state and the structure factor.

One such aspect of molecular models of mixtures that is poorly understood is the degree to which the cross-interaction deviates from strict Bertholet behavior. As a result, it is not surprising that models are often brought into agreement with experiment by adjusting this term. Since the bulk of the literature is based upon Flory−Huggins, or regular solution, theories of the solubility,[13] the non-Bertholet mixing term, l_{AB}, which is often associated with a polymer−gas pair, corrects for both deviations in the fundamental interactions and weaknesses in the traditional theories. In the current study, we also have speculated upon this aspect of the molecular models of the gas−polymer interaction.

2. Molecular Models

Both the CH_2 group in polyethylene and the gas molecules have been treated as single, spherical, Lennard-Jones sites with interactions given by

$$v(r) = 4\epsilon\left[\left(\frac{\sigma}{r}\right)^{12} - \left(\frac{\sigma}{r}\right)^{6}\right] \tag{2.1}$$

where ϵ is the well depth and σ is the Lennard-Jones diameter. This assumes a dispersive interaction, which, for many of the gases, is a good representation; however, for others, such as carbon dioxide and nitrogen, more complex behavior would be expected.

If the interactions were, in truth, dispersive, the cross-interaction between gas molecule A and polymer site B would also be of the Lennard-Jones form with ϵ_{AB} and σ_{AB} described by the Bertholet mixing rules:

$$\epsilon_{AB} = \sqrt{\epsilon_{AA}\epsilon_{BB}} \tag{2.2a}$$

and

$$\sigma_{AB} = (\sigma_{AA} + \sigma_{BB})/2 \tag{2.2b}$$

where ϵ_{AA}, ϵ_{BB}, σ_{AA}, and σ_{BB} are the potential parameters for gas−gas and polymer−polymer interactions.

For cases where the Lennard-Jones potential is suspected of being a crude approximation, either because of the nonspherical nature of the molecules or because of permanent dipole moments, Bertholet scaling would not be expected to hold. The most common way of formally accounting for non-Bertholet mixing is to introduce an additional parameter, l_{AB}, which varies the well depth of the cross-interaction from the geometric mean of those of the like interactions:

$$\epsilon_{AB} = (1 + l_{AB})\sqrt{\epsilon_{AA}\epsilon_{BB}} \tag{2.3}$$

The quantity l_{AB} also appears in the Flory−Huggins extension of regular solution theory to polymers; however, strictly speaking, it is not identical to the l_{AB} defined directly in terms of the potential interactions in eq 2.3. Instead, the l_{AB} in Flory−Huggins theory serves as a catchall for errors in the theory as well as for nondispersive effects. Consequently, it is, perhaps, not surprising that even benign cases, such as the noble gases, require nonzero l_{AB}'s in order to describe their solubilities in polyethylene with Flory−Huggins theory.[5]

In the current study, Bertholet mixing is assumed and standard Lennard-Jones potentials are used to describe the interactions between like species. As a result, any gas solubility measurements that deviate from the theoretical predictions would be interpreted as requiring a non-Bertholet model; however, for the limited experimental values of gas solubilities in completely amorphous polyethylene at room temperature, we find no clear evidence of non-Bertholet mixing.

For the preliminary comparison with simulation results, the intermolecular interaction potentials were the same as used in the simulation study. The gas potentials used were those of Gusev, Arizzi, and Suter[14] for argon, nitrogen, and oxygen, and of Sok and Berendsen[15] for methane. The CH_2 interaction was taken from Smit, Karaborni, and Siepmann.[16] The parameters for these potentials are listed in Table 1.

Four gas potential sets were investigated with the CH_2 potentials, and each of these was investigated with two different methods of calculating the hard sphere diameters. Two of the gas potential sets were determined in the traditional manners of using experimental viscosity and second virial coefficients. These were taken from the standard compilations of Hirschfelder, Curtiss, and Bird.[4] Table 2 lists their parameters.

Ben-Amotz and Herschbach[17] used the Carnahan−Starling−van der Waals (CS−vdW) equation of state to fit pressure−density isotherms. The CS−vdW equation of state relates the compressibility factor, Z, to the hard sphere diameter, d, and an attractive, van der Waals parameter, τ: $Z(d,\tau)$. Both d and τ were determined by fitting experimental points. Comparisons with simulation permitted the determination of the well depth, ϵ, and Lennard-Jones σ from τ and d. Their parameters are listed in Table 3.

The last set of gas potentials result from work by Matyushov and Schmid.[18] Their approach was similar

Table 1. Potential Parameters and Solubility Coefficient Ratio S_{PRISM}/S_{MD}(%) for Comparison with the Molecular Dynamics Study Reported by van der Vegt et al.[11]

gases	σ (Å)	ϵ (K)	S_{PRISM}/S_{MD}(BH)	S_{PRISM}/S_{MD}(WCA)
N_2	3.70	95	65 ± 9	87 ± 12
Ar	3.40	120	55 ± 6	67 ± 7
O_2	3.50	110	62 ± 7	94 ± 11
CH_4	3.73	150	69 ± 9	97 ± 12
CH_2	3.93	47		

Table 2. Gas Parameter Sets from Hirschfelder, Curtiss, and Bird[4]

	viscosity				second virial coefficient			
gas	σ (Å)	ϵ (K)	d_{WCA} (Å)	d_{BH} (Å)	σ (Å)	ϵ (K)	d_{WCA} (Å)	d_{BH} (Å)
N_2	3.681	91.5	3.56	3.47	3.698	95.05	3.58	3.49
Ar	3.418	124	3.35	3.25	3.405	119.8	3.33	3.24
O_2	3.433	113	3.35	3.26	3.58	117.5	3.50	3.40
CH_4	3.882	137	3.82	3.71	3.817	148.2	3.77	3.65
Kr	3.61	190	3.60	3.48	3.60	171.0	3.58	3.46
Xe	4.055	229	4.08	3.92	4.100	221	4.12	3.96
CO_2	3.996	190	3.99	3.84	4.486	189	4.48	4.32
C_2H_6	4.418	230	4.44	4.27	3.954	243	3.99	3.83

Table 3. Ben-Amotz and Herschbach[17] Gas Parameters

gas	σ (Å)	ϵ (K)	d_{WCA} (Å)	d_{BH} (Å)
N_2	3.67	96	3.56	3.46
Ar	3.41	117	3.33	3.23
CH_4	3.73	142	3.68	3.56
Kr	3.64	161	3.61	3.49
Xe	3.98	235	4.01	3.85
CO_2	3.69	247	3.72	3.57
C_2H_6	4.29	244	4.32	4.15

Table 4. Matyushov and Schmid[18] Gas Parameters

gas	σ (Å)	ϵ (K)	d_{WCA} (Å)	d_{BH} (Å)
N_2	3.63	102	3.53	3.43
Ar	3.37	120	3.30	3.20
O_2	3.34	116	3.26	3.17
CH_4	3.76	170	3.74	3.61
Kr	3.66	180	3.65	3.52
Xe	4.05	253	4.09	3.93
CO_2	3.77	242	3.80	3.65

Table 5. CH_2 Parameters and Hard Site Diameters

name	σ (Å)	ϵ (K)	d_{WCA} (Å)	d_{BH} (Å)
NERD[8]	3.93	45.8	3.67	3.60
TraPPE[9]	3.95	46.0	3.69	3.62

to that of Ben-Amotz and Herschbach in that the CS−vdW equation of state was used to determine hard sphere diameters. However, the Lennard-Jones parameters are determined from experimental solvation free energies. Embodied in their calculation was the assumption of a Barker−Henderson[19] (BH) decomposition of the potential. The parameters are listed in Table 4.

Using the given parameters, the potentials were decomposed in two ways: (1) using a Barker−Henderson division of the potential into repulsive and attractive contributions and (2) using a Weeks−Chandler−Andersen[20] (WCA) division. (These two approaches will be discussed shortly.) Tables 2−4 contain the potential parameters and both WCA and BH hard sphere diameters.

There is the possibility of a slight temperature dependence in the Lennard-Jones parameters. The parameters from Ben-Amotz and Herschbach are for 20 °C, those from Matyushov and Schmid are for 25 °C, and the sets from Hirschfelder et al. are collected from literature and have a wide temperature range. It is assumed that the change from 20 to 25 °C is small and that most of the parameters from Hirschfelder et al. are for temperatures close to 25 °C.

Because of chain connectivity, the modeling of the polyethylene melt is more difficult than that of the solute gas. The interatomic interactions considered in the current study are given by the Lennard-Jones parameters in Table 5.

In addition, the backbone structure of the polymer chains must be modeled. For this, the Koyama-patch description of Honnell et al.[21,22] is implemented for the site−site intramolecular probability distribution, $\Omega_{BB}(r)$. For sites separated by five or less bonds, the distribution is explicitly evaluated from the rotational isomeric state (RIS) model of Flory;[23] while, for larger separations, the distribution is approximated by a Koyama distribution that has second and fourth moments set equal to those of a RIS chain. Since the moments vary with the number of bonds separating the sites, the characteristic ratio smoothly changes from its short- to its long-ranged value. This proves to be an excellent description of the single chain distribution, as was shown by comparisons with neutron scattering.[21]

For the purposes of the calculation of gas solubilities, the distribution function of primary interest is the pair correlation function $g_{AB}(r)$ between the gas and polymer. The single chain distribution function is only indirectly needed as a feed to the PRISM theory which, in momentum space, is

$$\hat{H}_{\alpha\beta}(k) = \sum_{\sigma\lambda} \hat{\Omega}_{\alpha\sigma}(k)\, \hat{C}_{\sigma\lambda}(k)[\hat{\Omega}_{\lambda\beta}(k) + \hat{H}_{\lambda\beta}(k)] \quad (2.6)$$

where the carets denote Fourier space, $C_{\alpha\beta}(r)$ is the direct correlation function,

$$H_{\alpha\beta}(r) = \rho_\alpha \rho_\beta [g_{\alpha\beta}(r) - 1] \quad (2.7)$$

and

$$\Omega_{\alpha\beta}(r) = \frac{\delta_{\alpha\beta}\rho_\alpha}{N_\alpha} \sum_{ij} \omega_{ij}(r) \quad (2.8)$$

where N_α is the chain length, $\delta_{\alpha\beta}$ is the Kroneker delta, and $\omega_{ij}(r)$ is the normalized probability density between specific sites i and j on the same chain.

Computational ease suggests that the sites be treated as hard. In this case, $C_{\alpha\beta}(r)$ may be approximated as zero for separations greater than contact, and $g_{\alpha\beta}(r)$ is identically zero for smaller separations. As a result, the PRISM equations can be solved. The pressures for hard site systems are, of course, much higher than atmospheric. The addition of the attractions would, presumably, reduce the pressure to the experimental value; however, since the attractions will have little or no effect on the structure, the hard site PRISM calculations are sufficient for the present purposes.

In order for the sites to be approximated as hard, the Lennard-Jones potentials must be mapped onto a hard site diameter. This was done by separating the potential into attractive, $w(r)$, and repulsive, $u(r)$, components in two ways. First, following Weeks, Chandler, and Andersen[20] (WCA), one can write

$$u_{\alpha\gamma}(r) = v_{\alpha\gamma}(r) + \epsilon_{\alpha\gamma} \qquad r \le 2^{1/6}\sigma_{\alpha\gamma}$$
$$u_{\alpha\gamma}(r) = 0 \qquad r > 2^{1/6}\sigma_{\alpha\gamma} \quad (2.9a)$$

and

$$w_{\alpha\gamma}(r) = -\epsilon_{\alpha\gamma} \qquad r \le 2^{1/6}\sigma_{\alpha\gamma}$$
$$w_{\alpha\gamma}(r) = v_{\alpha\gamma}(r) \qquad r > 2^{1/6}\sigma_{\alpha\gamma} \quad (2.9b)$$

where $v_{\alpha\gamma}(r) = u_{\alpha\gamma}(r) + w_{\alpha\gamma}(r)$. The repulsive component then is associated with a hard site diameter by a Barker−Henderson[19] mapping

$$d_{\alpha\gamma} = \int_0^\infty \{1 - \exp[-\beta u_{\alpha\gamma}(r)]\}\, dr \quad (2.10)$$

which is roughly the point where the Mayer f-function of the repulsive potential has a value of one-half. This diameter is dependent only on temperature.

Second, the Barker−Henderson[19] perspective suggests that the potential be separated into reference and perturbation parts simply by

$$u_{\alpha\gamma}(r) = v_{\alpha\gamma}(r) \qquad r \le \sigma_{\alpha\gamma}$$
$$u_{\alpha\gamma}(r) = 0 \qquad r > \sigma_{\alpha\gamma} \tag{2.11a}$$

and

$$w_{\alpha\gamma}(r) = 0 \qquad r \le \sigma_{\alpha\gamma}$$
$$w_{\alpha\gamma}(r) = v_{\alpha\gamma}(r) \qquad r > \sigma_{\alpha\gamma} \tag{2.11b}$$

with the hard sphere diameter determined from the Barker−Henderson mapping of the reference potential (eq 2.10).

Since completely amorphous polyethylene is not an experimental reality at room temperature, its density must be determined indirectly. The *Polymer Handbook*[24] bases its prediction of 0.855 g/cm^3 on an extrapolation of the high-temperature measurements of Turner-Jones and Cobbold.[25] This agrees well with the extrapolation of alkane densities to the long chain limit (0.84 g/cm). It was the polyethylene density used both in the extrapolation of alkane gas solubility coefficients[5] and in the current study for comparisons with experimental measurements. The density and thermal expansion coefficient of high temperature, liquid polyethylene[26] can be used to yield a density of 0.900 g/cm^3 at 25 °C. For comparison with the simulations, a density of 0.848 g/cm^3 was used.

In addition to the difficulties of determining the density to be used, the assumptions underlying the calculation of $\Omega_{ab}(r)$ allows sites on ideal chains to occupy the same space as other sites. While the probability of this occurring is low, it cannot always be treated as negligible. To account for this overlap,[27] the density within the PRISM calculation of the $g(r)$ must be "bumped-up" by a factor of $1/(1 - \epsilon_N)$; however, the density used in the rest of the formalism is not altered. For the approximate form of the $\Omega_{ab}(r)$ used for polyethylene in the current study, this factor can be found[28] from

$$\frac{1}{1-\epsilon_N} = 1.0133 + 0.042242 \exp\left(\frac{-133.5}{N}\right) \tag{2.12}$$

where N is the number of sites on a chain. In this study, $N = 6429$ and the correction factor leads to an increased density of about 5.5%.

3. PRISM Theory of Gas Solubility

The PRISM methodology was developed by Schweizer and Curro[2] based upon the earlier work of Chandler and Andersen[29] on molecular liquids. The treatment of the additional complexities associated with long chain molecules was made possible by the random walk nature of polymers in the melt. The recent application of PRISM to gas solubility[1] parallels a similar study by Pratt and Chandler[30] of liquid−gas equilibrium in molecular fluids.

As with all equilibrium studies, the chemical potentials of each component in the two phases must be equated. For the case of small molecules dissolved in a polymer melt, the negligible vapor pressure of the polymer makes the small molecule, A, the only species whose chemical potential is of interest. The chemical potential of A in the gas phase, μ_A^G, is assumed to be given by the ideal gas expression,

$$\beta\mu_A^G = \ln[\beta P \Lambda^3] \tag{3.1}$$

where β is $1/kT$, P is the pressure, Λ is $h/\sqrt{2\pi mkT}$, k is the Boltzmann constant, h is Planck's constant, and m is the mass of the particles. It is relatively straightforward to include nonideal effects, important at higher pressures, from the equation of state.

On the other hand, the chemical potential of A in the polymer phase, μ_A^P, is more complex. It is conveniently viewed as the sum of three terms,

$$\mu_A^P = \mu_o + \Delta\mu_{ref} + \Delta\mu_H \tag{3.2}$$

where μ_o is the chemical potential of point particles in a volume V where polymers sites permit only $V(1 - \eta)$ of the space to be accessed. That is,

$$\beta\mu_o = \ln\left[\frac{\rho_A\Lambda^3}{(1-\eta)}\right] \tag{3.3}$$

where ρ_A is the number density of species A in the melt and η is the packing fraction. The inserted point particles then can be grown as hard sites to a diameter d_A. The associated reversible work, $\Delta\mu_{ref}$, is strongly affected by the changing pair correlation functions, $g_{AB}^{(\lambda)}(r)$, with the growth of the A particles as λ increases from 0 to 1. Explicitly, this is given by

$$\beta\Delta\mu_{ref} = \frac{\pi d_A \rho_B}{2}\int_0^1 d\lambda\, (d_B + \lambda d_A)^2 g_{AB}^{(\lambda)}\left(\frac{d_B + \lambda d_A}{2}\right) \tag{3.4}$$

where d_B is the hard site diameter of the polymer sites and d_A is that of the small molecules. The pair correlation functions are evaluated at contact as the molecules grow, and as a consequence, the integral must be performed numerically. Finally, since the g's are essentially unaffected by the attractive part of the potential, the contribution to the chemical potential of the attractions, $\Delta\mu_H$, is found through perturbation theory to be

$$\beta\Delta\mu_H = 4\pi\rho_B\int_0^\infty r^2 \beta w_{AB}(r)\, g_{AB}^o(r)\, dr \tag{3.5}$$

where $w_{AB}(r)$ is the attractive component of the potential interaction, and g_{AB}^o is the gas−polymer correlation function for the full-sized gas particle.

The Henry's law limit, as expressed by eqs 3.4 and 3.5, neglects gas−gas interactions within the polymer. A more general form would include g_{AA} correlation functions. More significantly, elevated gas concentrations, as would be expected with the more aggressive gases, would swell the polymer, thereby reducing the polymer's site density and affecting g_{AB}. Including such complexities in the PRISM treatment of solubility is, in principle, straightforward; however, additional computational complexities are introduced that are beyond the scope of the current study.

4. Results and Discussion

To evaluate the quantitative accuracy of theoretical predictions, either the results of simulations or experiments may be used for comparative purposes. Both

have advantages and disadvantages. In the case of simulations, the interaction potentials are known, and as a result, inaccuracies in the theoretical structure cannot be hidden by inaccuracies in the potentials. On the other hand, at least for realistic models of polymers, equilibration difficulties, due to finite simulation times, result in relatively large uncertainties in the prediction of certain properties and, for the case of solubility, limits the gases that can be studied. Furthermore, there is always the possibility that potentials selected for the simulations do not capture the full physics of the phenomenon under consideration.

The primary weakness in comparing theoretical to experimental results is the lack of knowledge of the true, underlying molecular model. Consequently, there are always inherent uncertainties in the potential interactions. On the other hand, experimental information is available from a broad range of systems and one is assured that the physical phenomenon is expressed in all its complexities.

In the current study, we are primarily interested in comparing to experimental results, but first, PRISM results are compared to those of the molecular dynamics study by van der Vegt et al.[11] This is of particular use in evaluating the relative accuracy of the BH and WCA decompositions of the potentials. While we do not use the same model of the chain backbone, both are "realistic" and, we assume, interchangeable to within the accuracy of the simulation and theory. A comparison of our PRISM calculations with their "slow compression with repulsive potentials" simulations is given in Table 1. The BH results are seen to be low (about 45%), and the WCA results, close to the values of simulation except for argon being fairly low. The selection of intermolecular potentials for comparisons with experimental results is a delicate matter. While one should avoid adjusting the potentials to fit the data, there is a wide range of potentials available in the literature that have been determined in manners independent of PRISM theory. The recently developed gas potentials of Matyushov and Schmid would be expected to perform well in this application, both because of the careful nature of their study and because solubility in liquids is taken into account. Unfortunately, an integral part of their study is the use of the BH potential decomposition which, to a degree, begs the question of the relative accuracy of the BH and WCA methods.

For the case of amorphous polyethylene, "experimental" results must be found from extrapolations of either liquid alkanes[5] or semicrystalline[6] polyethylenes. We have used the results of the former method. We have plotted the solubilities for natural rubber[6c] and both ways of extrapolating the solubility in polyethylene in Figure 1. Most of the differences between the alkane extrapolation and the natural rubber data are within the errors of the extrapolation to amorphous polyethylene, which we estimate to be roughly 15%.

Table 6 contains the results of all 16 solubility sets as ratios of PRISM to experimental[5] solubilities. The relative solubilities predicted using the same gas set but different separations do not show the trend of the one (either BH or WCA) always being greater than the other. This is a demonstration of the competing effects of size and attractiveness of a site. The larger the size of a site, the less soluble it is. On the other hand, the attractions show the opposite effect of the greater the attraction, the more soluble the site is. The WCA separation has a larger hard sphere diameter than the BH separation, but it also has a stronger attractive interaction.

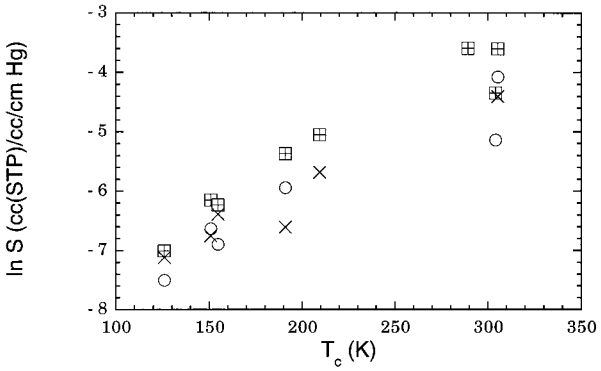

Figure 1. Solubility predictions of amorphous polyethylene as a function of the critical temperature of the gases. The crossed squares are for amorphous polyethylene found from alkane extrapolation;[5] the open circles, for the semicrystalline extrapolation.[6] The X's represent the natural rubber data from Michaels and Bixler.[6c]

Table 6. Comparison of Solubility with Experimental Data[5] as S_{PRISM}/S_{exp} (%)[a]

a. NERD CH_2 Potential[8]

gas	N_2	Ar	O_2	CH_4	Kr	Xe	CO_2	C_2H_6
T_c (K)	126	150.8	154.8	191	209.4	289.4	304	305.4
2HCB BH	119	126	115	78	104	58	47	97
2HCB WCA	135	119	106	72	99	70	60	88
BAH BH	129	122		64	81	82	184	86
BAH WCA	141	112		73	75	72	219	118
VHCB BH	110	135	112	53	146	70	69	71
VHCB WCA	124	127	106	66	143	59	58	64
MS BH	159	134	122	135	112	111	197	
MS WCA	146	122	136	127	100	97	191	

b. TRaPPE CH_2 Potential[9]

gas	N_2	Ar	O_2	CH_4	Kr	Xe	CO_2	C_2H_6
T_c (K)	126	150.8	154.8	191	209.4	289.4	304	305.4
2HCB BH	76	87	76	49	70	32	24	61
2HCB WCA	127	116	97	70	94	73	57	88
BAH BH	84	86		41	53	51	121	49
BAH WCA	133	109		67	71	72	226	129
VHCB BH	72	96	79	32	97	41	42	36
VHCB WCA	117	121	100	62	136	86	57	63
MS BH	106	97	87	87	74	65	129	
MS WCA	138	116	130	123	129	145	185	

[a] The first letters indicate the gas parameters with 2HCB = second virial coefficient of Hirschfelder, Curtiss, and Bird,[4] BAH = Ben-Amotz and Herschbach,[17] VHCB = viscosity of Hirschfelder, Curtiss, and Bird,[4] and MS = Matyushov and Schmid.[18] The final letters indicate the method of potential decomposition with BH = Barker−Henderson and WCA = Weeks−Chandler−Anderson.

It can be seen also that, although traditionally second virial coefficient parameters are used for thermodynamic properties that would include solubility,[31] in several cases the viscosity parameters more closely fit the "experimental" data.

Figures 2and 3 show the "best" gas fits to the alkane extrapolation data using both methods of potential separation. While it has been suggested that solubility be plotted in various ways to give a linear function,[6b,32,33] we have followed the traditional route of viewing the logarithm of the solubility coefficient as a nearly linear function of the critical temperature. Table 7 shows the results of the "best" gas potentials for each CH_2 potential. Oddly, argon and methane have some of the worst "best" fits even though they are expected to be modeled well by the Lennard-Jones single site potential. In

Table 7. Best Fit for Each Gas (Notation Same as Table 6)[a]

gas	T_c (K)	S_{PRISM}/S_{exp} (%)	WCA gas sets	S_{PRISM}/S_{exp} (%)	BH gas sets	experimental
			a. NERD CH_2 Potential[8]			
N_2	126	124	VHCB	110	VHCB	9.05E-04
Ar	150.8	112	BAH	122	BAH	2.13E-03
O_2	154.8	106	2HCB, VHCB	112	VHCB	1.96E-03
CH_4	191	127, 73	MS, BAH	78	2HCB	4.67E-03
Kr	209.4	100	MS	104	2HCB	6.41E-03
Xe	289.4	97	MS	111	MS	2.75E-02
CO_2	304	60	2HCB	69	VHCB	1.30E-02
C_2H_6	305.4	88	2HCB	97	2HCB	2.72E-02
			b. TRaPPE CH_2 Potential[9]			
N_2	126	117	VHCB	106	MS	9.05E-04
Ar	150.8	116	MS	97	MS	2.13E-03
O_2	154.8	100	VHCB	87	MS	1.96E-03
CH_4	191	123	MS	87	MS	4.67E-03
Kr	209.4	94	2HCB	97	VHCB	6.41E-03
Xe	289.4	86	VHCB	65	MS	2.75E-02
CO_2	304	57	2HCB, VHCB	121	BAH	1.30E-02
C_2H_6	305.4	88	2HCB	61	2HCB	2.72E-02

[a]Experimental[5] values of S are in units of cm(STP)/cm^3/cm Hg).

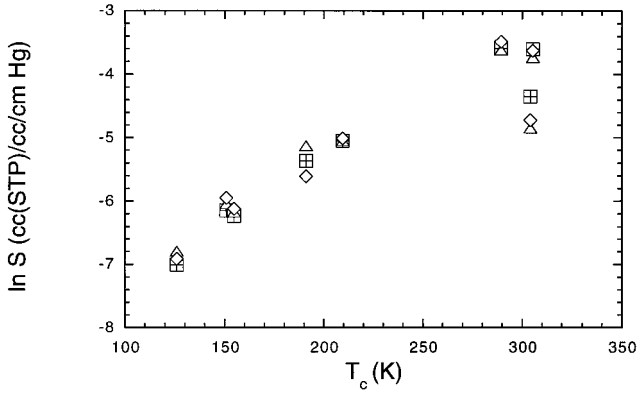

Figure 2. Solubility predictions for the best fit gases for the NERD potential.[8] The crossed squares are for amorphous polyethylene;[5] the triangles, for the WCA separation; the diamonds, for the BH separation. See Table 7a for the best fit values and gas set.

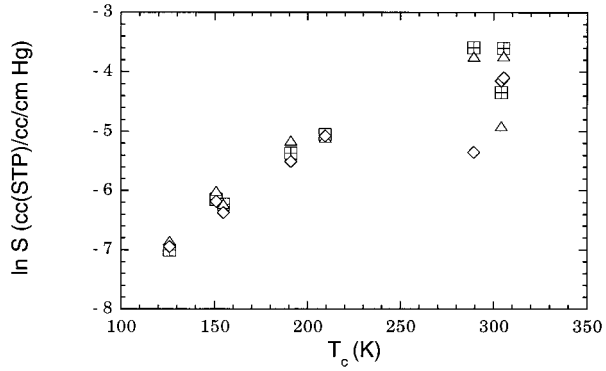

Figure 3. Solubility predictions for the best fit gases for the TRaPPE[9] potential. The crossed squares are for amorphous polyethylene;[5] the triangles, for the WCA separation; the diamonds, for the BH separation. See Table 7b for the best fit values and gas set.

addition, it can be seen that the MS potentials yield better predictions with the WCA decomposition than with the BH separation for the NERD potential; however, the 2HCB potentials give a better fit in many cases.

Intriguingly, although both CH_2 parameter sets have very similar values, the solubilities predicted in some cases are substantially different. Comparing between the two, the WCA separation generally gives similar results while the BH separation tends to give much different results. This implies that the WCA separation is the more robust decomposition methodology for solubility applications.

For all gas potentials, relatively good solubility coefficients were predicted without recourse to non-Bertholet mixing. On the other hand, the poorest agreement between PRISM and experiment was for nonspherical molecules, and one suspects that a more detailed, molecular treatment of these gases would improve matters. Such a refinement of PRISM theory is certainly possible, and work along this line is currently being pursued.

In summary, we have demonstrated in the current study that, from standard potential interactions, PRISM is capable of making reasonable predictions of room-temperature gas solubilities in rubbery polymers. Although, from a computational perspective, this is a more demanding treatment of solubility than traditional Flory−Huggins theory, it has the practical advantage of not requiring a hypothetical, pure, permeant liquid in coexistence with the gas phase. Furthermore, there is every reason to expect that (unlike the parameters necessary for the Flory−Huggins modeling of solubility) the atomic level interactions required in the PRISM treatment will be transferable between small molecule and polymer liquids.

References and Notes

(1) Curro, J. G.; Honnell, K. G.; McCoy, J. D. *Macromolecules* **1997**, *30*, 145. Note that eq 20b has an extraneous term of V in the denominator; the right-hand side of the equation should be the same as the first right-hand side term in eq 26. In eq 23, the integral limits should be the σ_{12}, which corresponds to the g_{12} for each integral. On p 150, the solubility equation should be $S = \phi/P = 1/K_H$.

(2) Schweizer, K. S.; Curro, J. G. *Phys. Rev. Lett.* **1987,** *58*, 246. Curro, J. G.; Schweizer, K. S. *Macromolecules* **1987,** *20*, 1928. Schweizer, K. S.; Curro, J. G. *Adv. Polym. Sci.* **1994,** *116*, 321. Schweizer, K. S.; Curro, J. G. *Adv. Chem. Phys.* **1997,** *98*, 1.

(3) Pierotti, R. A. *Chem. Rev.* **1976,** *76*, 721.

(4) Hirschfelder, J. O.; Curtiss, C. F.; Bird, R. B. *Molecular Theory of Gases and Liquids*; Wiley & Sons: New York, 1954.

(5) Budzien, J. L.; McCoy, J. D.; Weinkauf, D. H.; LaViolette, R. A.; Peterson, E. S. *Macromolecules* **1998**, *31*, 3368.

(6) (a) Michaels, A. S.; Parker, R. B. *J. Polym. Sci.* **1959,** *41*, 53. (b) Michaels, A. S.; Bixler, H. J. *J. Polym. Sci.* **1961,** *50*, 393. (c) Michaels, A. S.; Bixler, H. J. *J. Polym. Sci.* **1961,** *50*, 413.

(7) McCoy, J. D.; Mateas, S.; Zorlu, M.; Curro, J. G. *J. Chem. Phys.* **1995,** *102*, 8635.
(8) Nath, S. K.; Escobedo, F. A.; de Pablo, J. J. *J. Chem. Phys.* **1998**, *108*, 1.
(9) Martin, M. G.; Siepmann, J. I. *J. Phys. Chem. B* **1998**, *102*, 2569.
(10) See, for example: Van Amerongen, G. J. *J. Appl. Phys.* **1946,** *17*, 972. Kamiya, Y.; Mizoguchi, K.; Naito, Y.; Hirose, T. *J. Polym. Sci., Part B* **1986,** *24*, 535. Felder, R. M.; Huvard, G. S. *Methods of Experimental Physics*, *16c*; Academic Press: New York, 1980; pp 315−377.
(11) van der Vegt, N. F. A.; Briels, W. J.; Wessling, M.; Strathmann, H. *J. Chem. Phys.* **1996,** *105*, 8849.
(12) See, for example: Müller-Plathe, F.; Rogers, S. C.; van Gundersen, W. F. *J. Chem. Phys.* **1993,** *98*, 9895. Tamai, Y.; Tanaka, H.; Nakanishi, K. *Macromolecules* **1995,** *28*, 2544.
(13) See, for instance: Barton, A. F. M. *CRC Handbook of Solubility Parameters and Other Cohesion Parameters*, 2nd ed.; CRC Press: Inc., Boca Raton, FL, 1991.
(14) Gusev, A. A.; Arizzi, S.; Suter, U. W. *J. Chem. Phys.* **1993**, *99*, 2221.
(15) Sok, R. M.; Berendsen, H. J. C. *J. Chem. Phys.* **1992**, *96*, 4699.
(16) Smit, B.; Karaborni, S.; Siepmann, J. I. *J. Chem. Phys.* **1995**, *102*, 2126.
(17) Ben-Amotz, D.; Herschbach, D. R. *J. Phys. Chem.* **1990,** *94*, 1038.
(18) Matyushov, D. V.; Schmid, R. *J. Chem. Phys.* **1996,** *104*, 8627.
(19) Barker, J. A.; Henderson, D. *J. Chem. Phys.* **1967,** *47*, 4714.
(20) Weeks, J. D.; Chandler, D.; Andersen, H. C. *J. Chem. Phys.* **1971,** *54*, 5237.
(21) Honnell, K. G.; McCoy, J. D.; Curro, J. G.; Schweizer, K. S.; Narten, A. H.; Habenschuss, A. *J. Chem. Phys.* **1991,** *94*, 4659. McCoy, J. D.; Honnell, K. G.; Curro, J. G.; Schweizer, K. S.; Honeycutt, J. D. *Macromolecules* **1992,** *25*, 4905.
(22) Honnell, K. G.; Curro, J. G.; Schweizer, K. S. *Macromolecules* **1990,** *23*, 3496.
(23) Flory, J. P. *Statistical Mechanics of Chain Molecules*; Wiley: NewYork, 1969.
(24) Brandrup, J., Immergut, E. H., Eds. *Polymer Handbook*, 3rd ed.; John Wiley & Sons: New York, 1989.
(25) Turner-Jones, A.; Cobbold, A. J. *J. Polym. Sci. B* **1968**, *6*, 539.
(26) Olabisi, O.; Simha, R. *Macromolecules* **1975**, *8*, 206.
(27) Schweizer, K. S.; Curro, J. G. *J. Chem. Phys.* **1988**, *89*, 3350. Schweizer, K. S.; Curro, J. G. *Macromolecules* **1988**, *21*, 3070. Curro, J. G.; Schweizer, K. S.; Grest, G. S.; Kremer, K. *J. Chem. Phys.* **1989**, *91*, 1357. Honnell, K. G.; Curro, J. G.; Schweizer, K. S. *Macromolecules* **1990**, *23*, 3496.
(28) Honnell, K. G. Unpublished notes, 1988.
(29) Chandler, D.; Andersen, H. C. *J. Chem. Phys.* **1972,** *57*, 1930.
(30) Pratt, L. R.; Chandler, D. *J. Chem. Phys.* **1977,** *67*, 3683. Chandler D. In *Studies in Statistical Mechanics VIII*; Montroll, E. W., Lebowitz, J. L., Eds.; North-Holland: Amsterdam, 1982; p 274.
(31) See p 1110 in ref 4.
(32) Stern, S. A.; Charati, S. G.; Onurval, N. *J. Membr. Sci.* **1993**, *76*, 89.
(33) Stern, S. A.; Mullhaupt, J. T.; Gareis, P. J. *AIChE J.* **1969**, *15*, 64.

MA9803537